Submillimeter p-Ge Laser Using a Voigt-Configured Permanent Magnet

Kijun Park, Robert E. Peale, Henry Weidner, and Jin J. Kim

Abstract—**A p-Ge laser at 170–200 μm wavelengths in Voigt configuration using a regular permanent magnet is reported. Results are compared with those obtained using a Faraday-configured superconducting magnet. Emission is observed over a wider range of electric-field magnitude in Voigt configuration at a given magnetic field. Time-resolved emission studies reveal unusual pulse dynamics which depend on the magnitude and duration of the applied electric field. Spectral content, Gaussian-beam profiles, and polarization are essentially independent of these temporal effects. A significant repetition-rate increase is found using copper heat sinks. An increased emission-pulse delay with increasing initial-sample temperature and the temperature independence of the emission quench time are both explained by Joule heating of the laser medium. Lasing persists above 10 K, raising the possibility of a practical p-Ge laser without need for liquid helium as a coolant.**

I. Introduction

THE submillimeter/far-infrared wavelength region lacks adequate tunable-laser sources for potential applications such as remote sensing, molecular and solid-state spectroscopy, plasma diagnostics, and THz imaging. Free-electron lasers operate in the sub-mm region, but these are large and expensive facilities. The p-Ge laser, the only solid-state laser source in the 70–250 μm wavelength region [1], is a promising, compact, and potentially practical alternative [2]–[4].

A p-Ge laser is based on population inversion between light- and heavy-hole bands. An electric field (E) accelerates holes in a perpendicular magnetic field (B). Population inversion is achieved when E/B is tuned to prevent light holes from reaching the threshold for inelastic optical-phonon scattering while allowing heavy holes to do so. Light holes remain "hot" while heavy holes scatter back to $\mathbf{k} = 0$, where some of them become light holes. The laser wavelength is tunable over the broad gain region in k-space by use of a selective resonator [5]–[9]. The gain is homogeneously broadened [2], [7], [10] so that all the population inversion is available for emission at the wavelength selected.

We report multiline, narrow-band emission between 170 and 210 μm from a p-Ge laser in which a regular permanent magnet substitutes for the traditional superconducting magnet [11]–[15]. This provides an easier setup for the favorable Voigt configuration [16]–[18]. The temporal shape of the emission is studied using a fast detector, and some unusual pulse dynamics are revealed. Double-emission pulses appear at sufficiently high electric field and for sufficiently long electric-field pulse durations. Spectroscopy, beam profiles, and polarization studies reveal that the extra emission pulse contains no new spectral content or mode structure. For given field conditions, the delay of emission following electric-pulse initiation is temperature dependent, but the quenching of the emission pulse occurs at times independent of the initial-sample temperature. These temperature effects are explained by temperature-dependent gain creation and loss using a simple calculation of Joule-heating during the pulse. Copper heat sinks are shown to significantly increase the maximum repetition rate. Since these heat sinks could be cold fingers of a closed-cycle refrigerator, and since lasing is observed for initial lattice temperatures above 10 K, the possibility of a p-Ge laser entirely free of liquid helium is established.

II. Experimental Details

A 4.1 × 4.3 × 51 mm^3 p-Ge rod with Ga concentration of $N_A - N_D \sim 9 \times 10^{13}$ cm^{-3} (~33 ohm-cm) was cut out of a crystal grown by Eagle–Picher. It was placed between the poles of a permanent magnet or within a superconducting solenoid. The crystal was oriented so that $\mathbf{B} \parallel [001]$ and light propagation $\mathbf{k} \parallel [110]$ for Voigt geometry and $\mathbf{B} \parallel \mathbf{k} \parallel [110]$ for Faraday geometry. Electric pulses (~ 150 A, ~ 300 V) of ~ 1 μs duration were applied at 1 to 180 Hz through indium Ohmic contacts on the [110] faces (4.3 × 51 mm^2) using a high-power electric-pulse generator [19]. These orientations for Voigt geometry are new. The current was measured using a fast-current probe (Pearson, model 411) and the voltage was measured by using a high-voltage differential voltage probe (Tektronix, model P5200). The electric-field magnitudes are determined from the applied voltage divided by the distance between the Ohmic contacts. The end surfaces of the Ge rod were polished parallel to better than 1 arc-min as tested

Manuscript received October 13, 1995; revised March 1, 1996. This work was supported in part by internal funds provided by the Center for Research and Education in Optics and Lasers and by the University of Central Florida Division of Sponsored Research. Development of Event-locked Fourier Spectroscopy, used here in one of its first-ever applications, was funded by AFOSR Grant F49620-95-1-0075.

K. Park is with the Department of Electrical and Computer Engineering and the Center for Research and Education in Optics and Lasers, University of Central Florida, Orlando, FL 32816–2700 USA.

R. E. Peale is with the Department of Physics and the Center for Research and Education in Optics and Lasers, University of Central Florida, Orlando, FL 32816–2700 USA.

H. Weidner is with the Department of Physics, University of Central Florida, Orlando, FL 32816–2700 USA.

J. J. Kim is with the Department of Physics, the Department of Electrical and Computer Engineering, and the Center for Research and Education in Optics and Lasers, University of Central Florida, Orlando, FL 32816-2700 USA, and with the Center for Advanced Studies in Energy and Environment, Korea Electric Power Institute, Taejon, South Korea.

Publisher Item Identifier S 0018-9197(96)05027-0.

using HeNe laser reflections. We used a polished copper-back mirror. A copper mirror with a 1.5-mm-diameter hole or a 33.9-μm period #750 Cu mesh (8.6-μm wire) was used as the output coupler to complete the resonator. Both mirrors were insulated by 25-μm low-density polyethylene film to prevent electric discharge through them. Each magnet was attached to an insert for a variable temperature (2~300 K) cryostat (Janis 8DT) with ZnSe inner windows and high-density-polyethylene (HDPE) outer windows. Radiation was collected by a gold-coated off-axis ellipsoidal mirror and focused onto a Si-composite bolometer (Infrared Laboratories) or a Ge:Ga photoconductor (Tydex, Inc.) cooled to 4 K. The detector signal was processed by an oscilloscope and a digitizing camera. The light-path from the sample cryostat to the detector cryostat was evacuated to 0.1 Torr to prevent absorption by water vapor, though our Si bolometer still could be saturated easily by laser emission after 1 m travel through air. The temperature was determined using a calibrated Allen Bradley 1-kΩ carbon resistor mounted directly in contact with the Ge crystal. The free-space beam profiles were determined by stepping a 1-mm-wide slit across the outer window of the cryostat at about a 10-cm distance from the laser rod. Polarization studies used a wire-on-polyethylene polarizer from Harrick. Spectroscopy of pulsed-laser emission was performed with a continuously scanning Fourier-transform spectrometer (Bomem DA8) using a novel variant of interleaved data acquisition and a unique method of transforming the resulting interferograms [20]–[23].[1] For spectroscopic measurements at optimum field conditions for which the signal saturates the bolometer, 1 cm of teflon was used to attenuate the beam by ~10-fold.

A schematic of the permanent-magnet laser system is shown in Fig. 1. The magnets are made of 35–MG–Oe sintered $Nd_2Fe_{14}B$ alloy. The yoke and the poles, made of soft iron, are designed to concentrate magnetic flux through the Ge rod. The magnetic field within the sample volume is uniform within several percent as determined by finite-element analysis and measurement with a Hall probe. Sample and cryostat geometry constrain the permanent-magnet dimensions so that the current maximum field is 0.35 $\pm$ 0.01 T. Higher magnetic fields up to 4 T can be realized using larger permanent magnets, smaller samples, novel magnet configurations [24], and better magnetic materials such as cobalt iron and better NdFeB alloy. The Ge rod is placed between the magnet poles, with the output coupler on the bottom, so that the propagation of emission (k) is perpendicular to the magnetic field (Voigt geometry). In contrast, for the superconducting solenoid $\mathbf{B} \parallel \mathbf{k}$ (Faraday geometry). In both cases, a polished brass mirror reflects the emission horizontally out of the cryostat chamber.

III. Results

Fig. 2 shows emission intensity versus electric- and magnetic-field magnitude for the Faraday-configured p-Ge laser using the mesh-output coupler. These data are shown for comparison with earlier, well-known work on p-Ge lasers [2], [3]. In Fig. 2, we find strong signal for (0.5 kV/cm, 0.3 T)< (E, B) < (1.0 kV/cm, 0.8 T), and for (E, B) > (1.67 kV/cm, 1.3 T). The output intensity drops with an abrupt threshold-like behavior below our noise level outside the two field regions. The peak emission easily saturates the pre-amplifiers of the bolometer and the photoconductor so that the signal has to be taken directly at the detector output.

Both intensity and the width of the E, B ranges are very sensitive to the alignment and type of the cavity mirrors. Without mirrors, weak lasing has been observed due to internal reflection modes off the bare Ge surfaces [25], but we do not observe signal above our noise level under these conditions. The mesh output coupler produces more signal over a wider range of E and B than is achieved with the hole mirror, whose output-coupler losses are higher (higher transmission). If the

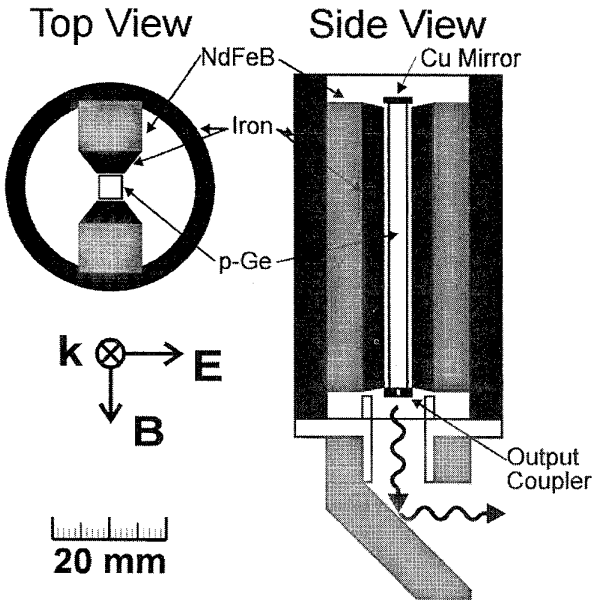

Fig. 1. Schematic of the p-Ge laser with a Voigt-configured permanent magnet. For the top view, the directions of the magnetic and electric fields applied to the sample and the propagation vector of the emission are shown.

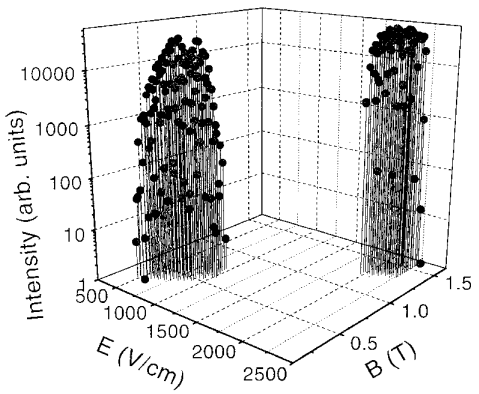

Fig. 2. Output intensity as a function of electric and magnetic fields for a p-Ge laser in Faraday configuration using a superconducting magnet. The mesh output coupler was used.

[1] This technique is available as a low-cost add-on to any Fourier-transform spectrometer from Zaubertek, Inc., 1007 Silcox Branch Circle, Oviedo, FL 32765 USA (407) 277-3795.

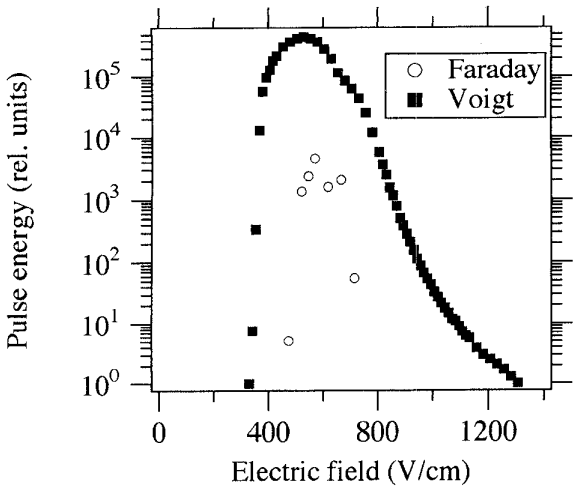

Fig. 3. Output intensity as a function of electric field for a p-Ge laser using a Voigt-configured permanent magnet and using a Faraday-configured superconducting magnet, $B = 0.35$ T.

end mirrors are purposely given a slight misalignment, the signal strength drops by five orders of magnitude to below our detection limit.

Fig. 3 compares Voigt- (permanent magnet) and Faraday-emission data as a function of applied electric field for the same 0.35-T magnetic field. The Ge rod and the cavity design are the same as for the experiment which produced the data in Fig. 2. We observe that our peak signal is two orders of magnitude stronger with the permanent magnet in Voigt configuration than with the superconducting magnet in Faraday configuration. Additionally, the electric-field range is significantly larger for the Voigt data. These observations are consistent with previous reports [16]–[18]. At electric-field values where the emission intensity begins to decrease, we nevertheless observe that the current density continually increases as the applied voltage is increased. Strictly speaking, this Voigt versus Faraday comparison is uncontrolled since the orientation of the magnetic field with respect to the crystal axes also differs for the two data sets. In similarly uncontrolled experiments, but with different field orientations, the intensity in Voigt configuration was larger by 20 to 30 times [17], [18].

The temporal behaviors of the current, applied voltage, and laser output (Voigt) at 4 K are shown in Fig. 4 for a range of electric-field strengths but for the same electric-field pulse duration. The numbers within each figure are the peak electric fields (V/cm) associated with each trace. The ringing in the beginning of the voltage pulse (and more weakly observed in the current trace) has a period roughly matching expectations for Gunn oscillations within the Ge [26], but they may also arise from imperfect matching of the pulse power supply with the low-impedence load. These oscillations are also observed in Faraday configuration. They disappear when the Ge crystal is replaced with a carbon resistor of similar value (several Ω). The oscillations at the end are due to the turn-off voltage surge in the pulse generator [19]. The noise generated by this turn-off is picked up by the detector as seen for times longer than 1.7 μs. This noise is observed even when the detector

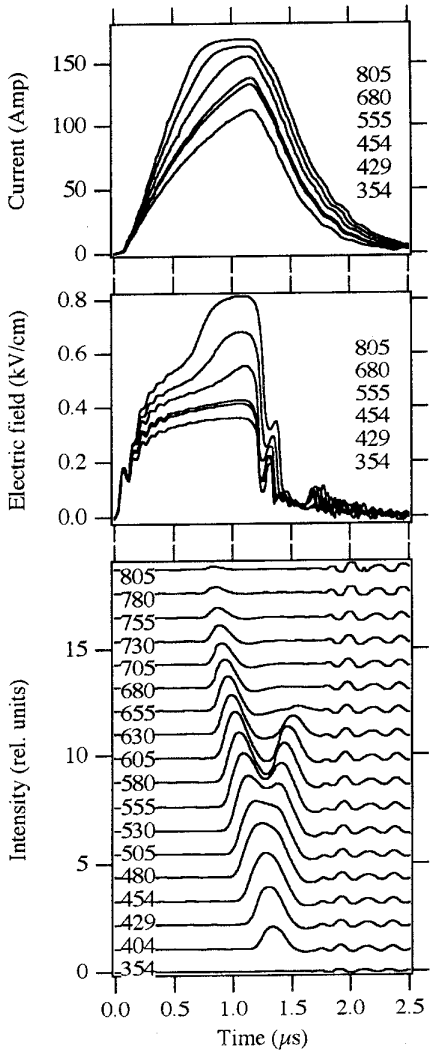

Fig. 4. Time dependence of the current and electric-field applied to the p-Ge rod and of the far-infrared emission. The numbers within each frame give the peak electric field in V/cm for the corresponding trace.

window is blocked, in which case the far-infrared signal is absent. An increase in current by 0.6% during the lasing is similar to a 2% increase reported by others [3], [10]. The rise and fall for the current are less abrupt than those for the voltage because of inductance in the leads, though effort has been expended to reduce inductance by use of straight, short, planar conductors.

Fig. 4 shows a rise time for the emission of about 100 ns, which is typical [4], [6], [27]–[29]. The rise of emission is significantly delayed from the initiation of the electric-field pulse. This delay depends on the field conditions. For low fields, a single-emission pulse occurs near the trailing edge of the voltage pulse. With increasing electric field, both the signal strength and its duration increase, and the initial rise moves to earlier times. Near the middle of the electric-field range, the pulse splits with the leading pulse continuing toward earlier times. The delay of the second peak increases until it moves beyond the termination of the voltage pulse. Both pulses

eventually decrease in strength as the electric field is increased, but the leading pulse persists to the highest electric field values. Others have published similar double-pulse traces without comment or comparison with the corresponding temporal behavior of the voltage and current [6].

Similar emission-pulse dynamics to Fig. 4 are observed if the pulse-generator's capacitor-charging voltage is kept constant but the pulse duration is increased. Fig. 4 reveals that the electric field needs time to reach its maximum value, so that the observed pulse-width dependence has arguably the same origin as its electric-field dependence. If voltage and current are continually applied for very long times (10–50 μs), a weak thermal-emission signal is eventually detected long after the high-intensity laser pulse has terminated.

Since the two emission pulses in Fig. 4 have differing electric-field dependences, they may also have differing spectral content, free-space beam profiles, or polarization dependence. To test this idea, and also to present important operating characteristics of the permanent magnet p-Ge laser, we have performed a number of measurements described next. In these measurements (Figs. 5–7, 10), the double pulse was obtained by lengthening the duration of the electrical pulse while keeping the charging voltage at the same value as for the single-pulse measurements.

Fig. 5 presents beam profiles for single- and double-pulse conditions using the mesh output coupler. The profiles are Gaussian, as revealed by the fits, and they have identical half-widths (FWHM) within experimental error. There is evidence of a side lobe, but its strength also appears independent of the details of the emission dynamics. The FWHM is 20% larger when the hole output coupler is used. The only previous reports [7], [30] of free-space beam profiles gave a lower divergence value of 1–1.5°, presumably because a semiconfocal resonator was used. Since these beams are within the $f/4$ optics of our detection system, the profiles can be measured even when the laser is imperfectly aimed at the detector, in which case better collection of the side lobe increases its relative strength. The Fig. 5 data indicate that the additional emission pulse introduces no new spatial modes to the beam.

Fig. 6 presents polarization data for the double-pulse condition using the mesh output coupler. The electric pulse had a peak field of 630 V/cm. Both pulses have their photon electric field highly polarized parallel to the applied electric field. When the field is reduced 25% by reducing the capacitor-charging voltage, single- and double-emission pulses obtained by changing pulse duration gave the same strong polarization as in Fig. 6. These data reveal that the second emission pulse introduces no modes of differing polarization and that the strong polarization observed is independent of applied electric field.

Fig. 7 presents spectra of the emission for single- and double-pulse conditions using the mesh output coupler. These spectra were collected using the slow bolometer, so they represent the time-integrated spectral content of the emission pulses. A 37-μm long-pass filter was used with the detector. Four major peaks appear in each spectrum. Since both spectra evidently have the same spectral content, the second emission pulse apparently does not introduce new frequencies. On the

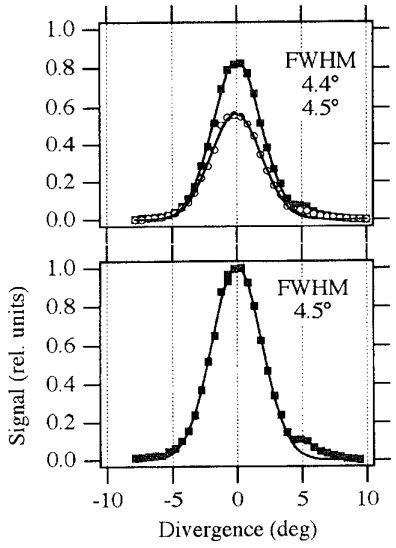

Fig. 5. Free-space beam profiles for double- and single-pulse conditions. The lines are Gaussian fits to the data. The crystal temperature is 4.2 K.

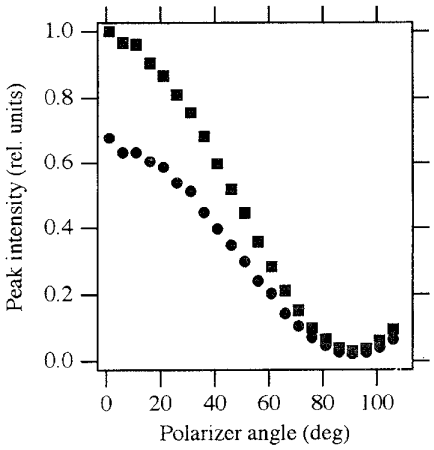

Fig. 6. Polarization dependence for each pulse in double emission-pulse conditions. Polarizer angle is measured with respect to the applied electric field. The lower curve corresponds to the later pulse.

contrary, the two weak outer groups are attenuated in the double-pulse spectrum relative to the central two peaks. This can be explained by mode competition because of the longer total duration of oscillation for the double pulse [6]. The resolution for the spectra in Fig. 7 was 0.2 cm^{-1}, and some linewidths in Fig. 7 are resolution limited. These data show that the spectral density of p-Ge emission is very high, as expected for a laser. This is in addition to having a total power output several orders of magnitude higher than usual spectroscopic broad-band thermal sources (globar) in the same frequency region, as determined by measurment using the same detector, optics, and spectrometer and by calculation (see Section IV).

Fig. 8 shows the temporal behaviors of the output intensity using the mesh output coupler for a number of different initial (pre-pulse) temperatures between 2 and 10 K, as measured with the fast Ge:Ga detector. These data were collected for

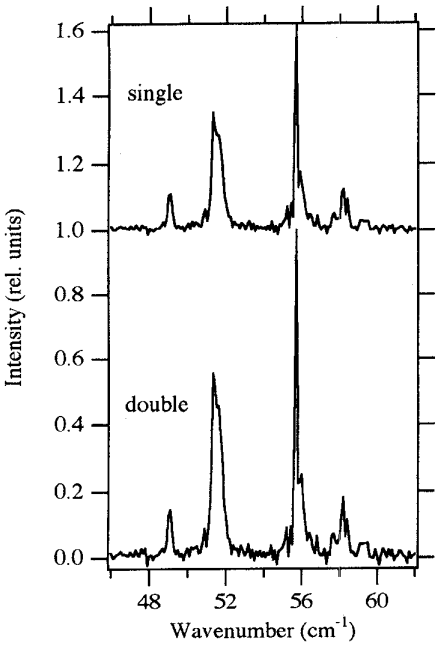

Fig. 7. Emission spectra for single- and double-pulse output. The resolution is 0.2 cm^{-1}.

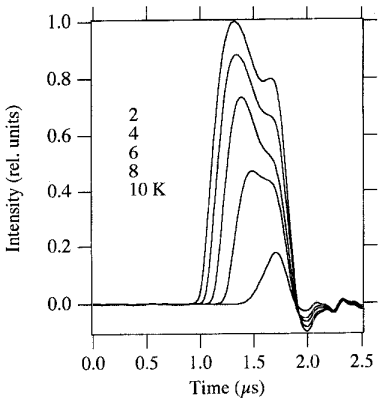

Fig. 8. Temperature-dependent emission-pulse dynamics. The zero of the time scale corresponds to the electric-pulse initiation.

peak electric fields of about 0.5 kV/cm. To our knowledge, these are the first reported p-Ge laser results below 4.2 K. Signal persists for initial-sample temperatures beyond 10 K. Use of the hole output coupler under otherwise identical conditions gives emission only up to 5 K. Increasing the initial-sample temperature increases the delay of the laser pulse. Normalizing each curve by its peak value reveals that the rise time increases slightly with increasing initial temperature, indicating a decrease in net small-signal gain. There is apparently no dependence on the initial crystal temperature for the emission-quench dynamics.

Fig. 9 presents the temperature dependence of the total output energy down to 1.7 K. These data were obtained by integrating the pulse profiles in Fig. 8. The time-integrated signal drops steadily with increasing temperature, but signal persists beyond 10 K, as mentioned already.

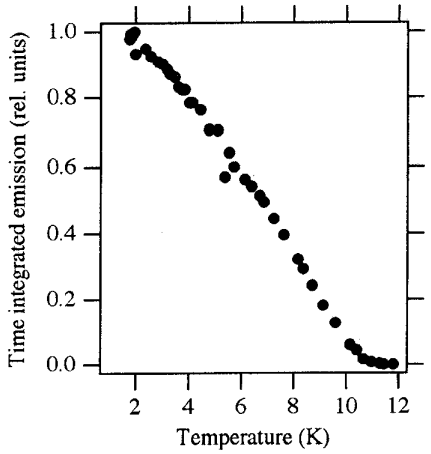

Fig. 9. Integrated emission-pulse intensity versus temperature.

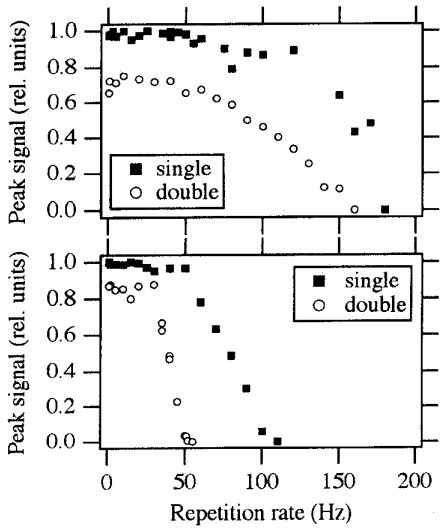

Fig. 10. Peak signal versus repetition rate with (top) and without copper heat sinks. Comparison is made also between single- and double-emission pulse conditions.

Fig. 10 shows the output intensity vs. repetition rate at 4.2 K. The upper plot gives peak signal using Cu heat sinks while the lower plot presents the same without. The heat sinks evidently increase the maximum repetition rate by a factor of about 2. Repetition rates are also higher for the single rather than the double pulse, for which each pulse has the same repetition-rate dependence. An independent study [31] shows that even higher repetition rates can be achieved by lowering the hole concentration and by using miniature crystals, at the expense of output power. Our heat sinks double as electrodes.

IV. Discussion

Figs. 7–9 reveal several interesting effects in the temperature dependence of the pulse dynamics. These include the temperature-dependent delay and the common quench dynamics for all initial temperatures. To gain insight, we calculated the lattice temperature rise during the electric pulse

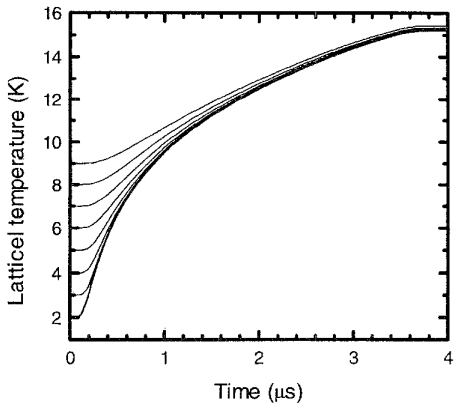

Fig. 11. Simulation of Ge-lattice temperature rise under Joule heating with no cooling. Initial lattice temperatures are between 2 K and 9 K. The heating turns off at 3.6 μs.

using a simple Joule heating model with no cooling. The assumption of no cooling was made because the cooling-time constant is orders of magnitude longer than the electric-pulse duration. This assertion is supported by calculation and by the repetition rate data (Fig. 10), where a thermal time constant of approximately 1/100 Hz = 10 ms is inferred. The equation

$$\int_{T_0}^{T} C(T)dT = \int_{0}^{t} I(t)V(t)dt$$

was solved numerically for temperature T versus time t given initial temperature T_0. The measured (e.g., Fig. 4) instantaneous electrical power $I(t)V(t)$ was used together with the experimental heat capacity $C(T)$ of Ge [32]. The calculated temperature rise during the electric pulse is shown in Fig. 11 for usual field conditions but for pulse durations of 3.6 μs.

Increasing temperature increases the population of acoustic phonons, which adversely affect lasing in two ways. First, via elastic scattering they disrupt the anisotropic-momentum distribution needed to establish and maintain a population inversion [2]. Second, acoustic phonons absorb the FIR emission [33] and so constitute a loss. Establishment of the threshold conditions will occur later if the pumping mechanism is less efficient and if losses are higher, which explains the increasing emission delay with increasing initial-sample temperature (Fig. 8).

The temperature versus time curves in Fig. 11 are almost independent of T_0 at times when the emission pulse terminates. At these times, therefore, the disruption of pumping by elastic scattering and the absorption loss will have reached levels independent of their lower initial values. In other words, the time at which loss exceeds gain should be independent of the starting temperature. This explains the universal quench dynamics observed in Fig. 8.

The observed emission delay implies a time of about 1 μs to establish a significant population inversion. Hence, the number of times a given hole can contribute a photon to the laser pulse is on the order of unity, since the whole pulse is over by 2 μs. Assuming impact ionization is complete, there are about 10^{14} free holes in the sample during the lasing. If each contributes one 200-μm photon to the pulse, the pulse energy is 100 nJ, giving a full-width-half-maximum power of 100 mW for a 1-μs pulse.

Laser-output power at 200 μm is difficult to measure accurately. The sensitivity figure provided with the Ge:Ga photoconductor gives a peak-power level of 0.5 mW. The power output can also be estimated from the time-integrated bolometer voltage using a slow-chop sensitivity figure (volts per Watt) provided by the manufacturer. This estimate gives a pulse energy of about 1 nJ, or a power of 1 mW for a 1-μs pulse. However, the modest bolometer-preamp bandwidth (<kHz) clips the initial voltage rise. By estimating the peak voltage for infinite preamp bandwidth from an extrapolation to zero time of the long-time exponential voltage decay, we find that the actual emission power could easily be as much as 100 mW. This value is in agreement with the crude power estimate from pulse-dynamics considerations in the previous paragraph. Passage of our beam through 3 cryostat windows can easily cause a ten-fold reduction in the measured power. Other workers have reported peak powers as high as 10 W [2].

A few far-infrared specialists remain skeptical that laser oscillation occurs as claimed in p-Ge. Instead, a thermal-radiator explanation is proposed, since a considerable amount of electrical energy is dissipated in the crystal during each shot. To argue against this interpretation, we collect here all of the evidence for lasing existing in this paper. In addition, we mention some results of others.

In Fig. 2, the field domains where lasing occurs agree with the accepted pumping mechanism for intervalence-band stimulated emission in p-Ge and with the observations of previous workers [2]. The sharp electric- (Figs. 2 and 3) and magnetic-field (Fig. 2) threshold behaviors are characteristic of pumping thresholds for lasers but not of thermal radiators. The strong dependences of the signal strength, field-domain size, and temperature range on end-mirror alignment and output-coupler reflectivity are explained in terms of feedback and output-coupler losses as for lasers, but such a dependence is unexpected for thermal radiators. A thermal-radiator model cannot explain the observed sub-μs emission-pulse dynamics (Fig. 4), since the thermal time constant of the crystal is approximately 10 ms. A delay of emission followed by a fast onset after pump initiation (Figs. 4 and 8) are both laser characteristics, since time is needed to establish sufficient population inversion after which emission rises exponentially [34]. A small signal gain of 0.1 cm^{-1} has been measured directly via amplification of an FIR gas-laser beam by passage through a p-Ge crystal during the first 0.1 μs of pumping [10], whereas a thermal radiator would not similarly amplify an external optical signal.

The observed high degree of polarization (Fig. 6) would be improbable for thermal radiation. In previous Voigt studies [16], [17], the degree and direction of polarization for a given emission line varied strongly with magnetic and electric field. These effects were explained by invoking an anisotropic absorption process due to the anisotropic-momentum distribution of holes including cyclotron motion. Alternatively, the strong linear polarization we observed for the few field

strengths tested can be explained in terms of low-loss cavity modes. For oblique internal-reflection modes [25], reflections from the contacted surfaces will be lossy, and the reflection coefficient below the critical angle at the clean faces is higher for polarizations perpendicular to the plane of incidence, i.e., parallel to the applied electric field.

Even though peak electrical power in the crystal can reach 50 kW, Fig. 11 shows that by the end of the emission pulse at approximately 2 μs, the sample has attained a temperature of only about 12 K, even without cooling. Experimental observations support a similarly low value for the final temperature. For such temperatures, assuming the Ge is a perfect, uniformly radiating black body, the Stefan–Boltzmann law and geometrical considerations show that the thermal radiation collected by the detector will be less than 1 nW. Since our power estimate is between 0.5 and 100 mW, and since many other workers [2] have reported up to 10 W, the observed signal is stronger by many orders of magnitude than expectations for a 12-K thermal radiator. For comparison, the ~1200-K globar we use for FIR spectroscopy sends less than 3 μW to our detector below 100 cm^{-1}. Our spectra (Fig. 7) reveal linewidths less than 0.2 cm^{-1}, so the spectral density is many orders of magnitude larger than for usual broad-band black-body sources. Heterodyne mixing of p-Ge and gas-laser radiation reveals laser modes with MHz line widths [9]. Beating between such modes has also been reported [29]. The spectral density can be increased by four orders of magnitude while maintaining the same total output power by means of a selective resonator [9]. This behavior is characteristic of lasers with a homogeneously broadened band and not of thermal radiators.

The thermal-radiator model also fails to explain the strong dependence on the initial crystal temperature (Fig. 9). The detectors are ac coupled and will measure only a change in black-body emission. As initial temperature increases, the rapid increase in black-body emission (Stefan–Boltzmann law) is offset by a decreased temperature change (higher initial specific-heat). Calculation shows that the change in thermal radiation depends only weakly on the initial-sample temperature.

Cooling efficiency, though neglected in the simulation of temperature rise (Fig. 11), clearly effects the thermal time constant of Ge and thus limits the repetition rate. After 1 μs of electrical excitation, the temperature of Ge rod is above 9 K (Fig. 11) and is surrounded and insulated by gas. Thermal anchoring of the Ge to Cu provides a good heat sink and improves cooling efficiency since the thermal conductivity of Cu is more than three orders of magnitude larger than He at 4 K [35]. This effect gives the observed repetition-rate increases (Fig. 10).

The copper heat sinks could also serve as electrodes and as cold fingers of a closed-cycle refrigerator, which can reach temperatures where lasing is still observed (Fig. 9). Commercial models are now available (e.g., Balzers) which provide 0.5 W of cooling power at 4.2 K. For normal p-Ge operating conditions, i.e., 50 kW of electric power in 1-μs pulses at a 10-Hz repetition rate, the average Joule-heat load is 0.5 W.

V. Summary

We have demonstrated a novel p-Ge laser near 200-μm wavelength using a regular Voigt-configured permanent magnet for the first time. Unusual pulse dynamics are observed as a function of applied electric field. These temporal effects appear to affect only the intensity and not the beam profile, polarization, or spectral content of the emission. Observed temperature dependent pulse dynamics were explained in terms of Joule heating with temperature dependent gain creation and loss. Large Cu heat sinks are made possible by the open permanent-magnet architecture and significantly increase the repetition rate. The heat sinks could also serve as cold fingers of a closed cycle refrigerator. By thus eliminating liquid helium, p-Ge lasers would become significantly more attractive as a practical source in a wavelength range where there is still no solid-state alternative.

References

[1] E. R. Brown, K. A. McIntosh, K. M. Nichols, M. J. Manfra, and C. L. Dennis, "Optical-heterodyne generation in low-temperature-grown GaAs up to 1.2 THz," *SPIE,* vol. 2145, pp. 200–208, 1994.

[2] E. Gornik and A. A. Andronov, Eds., *Far-Infrared Semiconductor Lasers.* Special issue of *Opt. Quantum Electron.*, vol. 23, no. 2, 1991.

[3] A. A. Andronov, Ed., *Submillimeter Wave Lasers Based on Hot Holes in Semiconductors.* Gorky, USSR: Inst. of Appl. Phys., Academy of Sciences of USSR, 1986 (in Russian).

[4] E. Bründermann, H. P. Röser, and M. F. Kimmitt, "Tunable p-germanium monocrystal laser for the wavelength region from 70 μm to 350 μm," *Laser und Optoelektronik*, vol. 25, pp. 48–60, 1993.

[5] S. Komiyama, H. Morita, and I. Hosako, "Continuous wavelength tuning of inter-valance-band laser oscillation in p-type Germanium over range of 80–120 μm," *Jpn. J. Appl. Phys.*, vol. 32, pp. 4987–4991, 1993.

[6] A. V. Murav'ev, I. M. Nefedov, S. G. Pavlov, and V. N. Shastin, "Tunable narrowband laser that operates on interband transitions of hot holes in germanium," *IEEE J. Quantum Electron.*, vol. 23, pp. 119–124, 1993.

[7] L. E. Vorobjev, S. N. Danilov, D. V. Donetskil, Yu. V. Kochegarov, V. I. Stafeev, and D. A. Firsov, "Noninjection narrow-band laser emitting far-infrared radiation due to hot holes and its use in impurity breakdown investigations," *Semicond.*, vol. 27, pp. 77–82, 1993.

[8] A. A. Andronov, V. A. Kozlov, S. A. Pavlov, and S. G. Pavlov, "External Bragg selection in a hot-hole germanium semiconductor laser," *Sov. J. Quantum Electron.*, vol. 20, pp. 1211–1213, 1990.

[9] E. Bründermann, H. P. Röser, A. V. Muravjov, S. G. Pavlov, and V. N. Shastin, "Mode fine structure of the p-Ge intervalence band laser measured by heterodyne mixing spectroscopy with an optically pumped gas laser," *Infrared Phys. Technol.*, vol. 36, pp. 59–69, 1995.

[10] F. Keilmann and H. Zuckermann, "Transient gain of the germanium hot hole laser," *Opt. Commun.*, vol. 109, pp. 296–303, 1994.

[11] K. Park, H. Weidner, R. E. Peale, J. J. Kim, and E. E. Haller, "A table-top 100 μm laser," in *Advanced Solid-State Lasers, 1995 Tech. Dig.* Washington, DC: Opt. Soc. Amer., pp. 242–244.

[12] ——, "Sub-mm p-Ge laser using a regular permanent magnet," *OSA Proc. Adv. Solid-State Lasers*, B. H. T. Chai and S. A. Payne, Eds., Washington, DC, vol. 24, pp. 277–281, 1995.

[13] K. Park, R. E. Peale, H. Weidner, and J. J. Kim, "Sub-mm p-Ge laser using a permanent magnet in Voigt configuration," *Proc. SPIE-Int. Conf. Millimeter and Submillimeter Waves and Applications II,* San Diego, CA, vol. 2558, pp. 312–318, 1995.

[14] ——, "Far-infrared p-Ge laser: Temperature dependent laser dynamics," in *Advanced Solid-State Lasers, 1996 Tech. Dig.* Washington, DC: Opt. Soc Amer., pp. 277–281.

[15] R. E. Peale, K. Park, H. Weidner, and J. J. Kim, "Far-infrared p-Ge laser: Pulse dynamics and repetition-rate enhancement," to be published in *Advanced Solid-State Lasers, 1996 Tech. Dig.* Washington, DC: Opt. Soc. Amer.

[16] I. Hosako and S. Komiyama, "p-type Ge far-infrared laser oscillation in Voigt configuration," *Semicond. Sci. Technol.*, vol. 7, pp. B645–B648, 1992.

[17] L. E. Vorobjev, S. N. Danilov, D. V. Donetsky, D. A. Firsov, Y. V. Kochegarov, and V. I. Stafeev, "An injectionless FIR laser based on interband transitions of hot holes in germanium," *Semicond. Sci. Technol.*, vol. 9, pp. 641–644, 1994.
[18] L. E. Vorobjev, S. N. Danilov, and V. I. Stafeev, "Generation of far-infrared radiation by hot holes in germanium and silicon in $E \times H$ fields," *Opt. Quantum Electron.*, vol. 23, no. 2, pp. S221–S229, 1991.
[19] K. Park and J. J. Kim, "A high power current pulse generator using an insulated-gate bipolar transistor," *Rev. Sci. Instrum.*, vol. 66, pp. 3713–3714, 1995.
[20] H. Weidner and R. E. Peale, "Time resolved Fourier spectroscopy for activated optical materials," *Appl. Opt.*, 1996, in press.
[21] H. Weidner, C. J. Schwindt, and R. E. Peale, "Time resolved Fourier spectroscopy for phosphor characterization," *J. Soc. Information Display*, Nov. 1995, submitted for publication.
[22] H. Weidner and R. E. Peale, "Event-locked time-resolved Fourier spectroscopy," *Appl. Spectrosc.*, 1996, submitted for publication.
[23] ——, "A powerful new technique for laser crystals: Time-resolved Fourier spectroscopy," in *Advanced Solid-State Lasers, 1996 Tech. Dig.* Washington, DC: Opt. Soc. Amer., pp. 340–342.
[24] H. A. Leupold, A. S. Tilak, and Ernest Potenziani, II, "Adjustable multi-tesla permanent magnet field sources," *IEEE Trans. Magn.*, vol. 29, pp. 2902–2904, 1993.
[25] K. Unterrainer, M. Helm, E. Gornik, E. E. Haller, and J. Leotin, "Mode structure of the p-germanium far-infrared laser with and without external mirrors: Single line operation," *Appl. Phys. Lett.*, vol. 52, p. 564, 1988.
[26] I. V. Altukhov, M. S. Kagan, K. A. Korolev, and V. P. Sinis, "Electrical domains and far-IR emission in uniaxially deformed p-Ge," *JETP*, vol. 76, pp. 903–909, 1993.
[27] S. Komiyama and S. Kuroda, "Far-infrared laser oscillation in p-Ge," *Solid State Commun.*, vol. 59, pp. 167–172, 1986.
[28] F. Keilmann and R. Till, "Saturation spectroscopy of the p-Ge far-infrared laser," *Opt. Quantum Electron.*, vol. 23, no. 2, pp. S231–S246, 1991.
[29] A. V. Bespalov, "Temporal and mode structure of the interband p-germanium laser emission," *Appl. Phys. Lett.*, vol. 66, pp. 2703–2705, 1995.
[30] L. E. Vorobjev, S. N. Danilov, D. V. Donetsky, D. A. Firsov, Yu. V. Kochegarov, and V. I. Stafeev, "Narrow band tunable sub-millimeter hot hole injectionless semiconductor laser and its use for cyclotron resonance investigation," *Opt. Quantum Electron.*, vol. 25, pp. 705–721, 1993.
[31] E. Bründermann, H. P. Röser, W. Heiss, E. Gornik, and E. E. Haller, "High repetition rate far-infrared p-type germanium hot hole lasers," *Appl. Phys. Lett.*, vol. 67, p. 3543, 1995.
[32] P. Flubacher, A. J. Leadbetter, and J. A. Morrison, "The heat capacity of pure silicon and germanium and properties of their vibrational frequency spectra," *Philos. Mag.*, vol. 4, pp. 273–294, 1959.
[33] R. Brazis and F. Keilmann, "Light absorption of Ge in the far infrared," *Solid State Commun.*, vol. 70, pp. 1109–1111, 1989.
[34] A. E. Siegman, *Lasers*. Mill Valley, CA: Univ. Science, 1986, ch. 6, p. 260.
[35] A. C. Rose-Innes, *Low Temperature Techniques*. London, U.K.: English Univ. Press, 1964, p. 147.

Kijun Park was born in Inchon, South Korea, in 1968. He received the B.S. degree in applied physics from Inha University, Inchon, South Korea, in 1991 and the M.S. degree in optical science and engineering from the University of Central Florida, Orlando, FL, in 1993. He is working towards the Ph.D. degree in optical sciences and electrical engineering at the Center for Research and Education in Optics and Lasers at the University of Central Florida.

His research interests include far-infrared and Terahertz-wave optics, tunable semiconductor and solid-state lasers, and computer-generated holograms.

Mr. Park is a member of the Optical Society of America.

Robert E. Peale received the B.A. degree in physics from the University of California, Berkeley, in 1983 and the Ph.D. degree in physics in 1990 from Cornell University, Ithaca, NY.

While at Cornell, he studied defects in semiconductors by FIR and IR spectroscopy. As a Research Associate at Lehigh University, Bethlehem, PA, he studied the magnetooptical properties of DX centers in bulk AlGaAs. Upon becoming an Assistant Professor at the University of Central Florida, Orlando, in 1991, he initiated work on FIR semiconductor lasers.

Henry Weidner received the Diplom in physics from Friedrich-Schiller-Universitat Jena in 1991 and is working towards the Ph.D. degree in physics at the University of Central Florida, Orlando. He has made a significant contribution to the use of continuously scanning Fourier spectrometers in studying transient events with ns-to-ms time scales in the FIR to UV spectral range. He is now commercializing a low cost add-on which adds time-resolving capability to any continuously scanning Fourier spectrometer.

Jin J. Kim, photograph and biography not available at the time of publication.